Structure
Article

Structural Insights into the Recruitment of SMRT by the Corepressor SHARP under Phosphorylative Regulation

Suzuka Mikami,[1,4] Teppei Kanaba,[1,4] Naoki Takizawa,[2,4] Ayaho Kobayashi,[1,4] Ryoko Maesaki,[1,3] Toshinobu Fujiwara,[2,5] Yutaka Ito,[1] and Masaki Mishima[1,*]
[1]Graduate School of Science and Engineering, Tokyo Metropolitan University, 1-1 Minamiosawa Hachioji 192-0397, Japan
[2]Institute of Microbial Chemistry, Tokyo 3-14-23 Kamiosaki, Shinagawa-ku 141-0021, Japan
[3]Graduate School of Bioscience, Nara Institute of Science and Technology, 8916-5 Takayama, Ikoma, Nara 630-0192, Japan
[4]These authors contributed equally to this work
[5]Present address: Graduate School of Pharmaceutical Sciences, Nagoya City University, 3-1 Tanabe-dori, Mizuho-ku, Nagoya 467-8603, Japan
*Correspondence: mishima-masaki@tmu.ac.jp
http://dx.doi.org/10.1016/j.str.2013.10.007

SUMMARY

The transcriptional corepressors SMRT/NCoR, components of histone deacetylase complexes, interact with nuclear receptors and many other transcription factors. SMRT is a target for the ubiquitously expressed protein kinase CK2, which is known to phosphorylate a wide variety of substrates. Increasing evidence suggests that CK2 plays a regulatory role in many cellular events, particularly, in transcription. However, little is known about the precise mode of action involved. Here, we report the three-dimensional structure of a SMRT/HDAC1-associated repressor protein (SHARP) in complex with phosphorylated SMRT, as determined by solution NMR. Phosphorylation of the CK2 site on SMRT significantly increased affinity for SHARP. We also confirmed the significance of CK2 phosphorylation by reporter assay and propose a mechanism involving the process of phosphorylation acting as a molecular switch. Finally, we propose that the SPOC domain functions as a phosphorylation binding module.

INTRODUCTION

SMRT/HDAC1-associated repressor protein (SHARP) is a transcriptional corepressor that was identified independently in nuclear receptor and Notch/RBP-Jκ signaling pathways (Oswald et al., 2002; Shi et al., 2001). SHARP is characterized by N-terminal RNA recognition motifs (RRMs) and a highly conserved C-terminal Spen paralog and ortholog C-terminal (SPOC) domain. The RRM domains of SHARP bind the steroid hormone receptor activator (SRA) (Newberry et al., 1999; Shi et al., 2001), which is emerging as a functional RNA acting as both noncoding RNA and coding RNA (Colley and Leedman, 2011; Cooper et al., 2011; Lanz et al., 2002; Novikova et al., 2012). SRA itself is a coactivator for transcription regulated by the nuclear hormone receptor, and SRA protein (SRAP) coded by SRA acts as a corepressor of SRA. The SPOC domain of SHARP directly interacts with the transcriptional corepressors silencing mediator for retinoid and thyroid receptor (SMRT)/nuclear receptor corepressor (NCoR), which are well-known components of HDAC complexes. Via SMRT/NcoR, SHARP recruits HDAC and thus represses transcription. Transactivation by the glucocorticoid receptor and estrogen receptor is thought to exert negative feedback via the expression of SHARP (Shi et al., 2001).

SMRT and NCoR are large corepressors and are considered to be unstructured for the most part, share high similarity, and interact with multiple transcriptional factors and coregulators. They act as "platform proteins" in recruiting a corepressor complex (Watson et al., 2012a). The N-terminal regions of SMRT/NCoR bind to both transducin beta-like protein 1 (TBL1) and G protein pathway suppressor 2 (GPS2), forming a three-way complex that represents the core of a multimeric structure (Oberoi et al., 2011). The LSD motif, located at the acidic C-terminal tail of SMRT/NCoR, was suggested as being responsible for binding to the SPOC domain of SHARP (Ariyoshi and Schwabe, 2003; Shi et al., 2001). In addition, it was shown that the second residue (Ser) of the LSD motif is a phosphorylation site for CK2, which is reported to be phosphorylated in cells (Olsen et al., 2006; Zhou et al., 2001). Nevertheless, little is known about the role of this phosphorylative event.

As a signaling protein, CK2 is a promiscuous kinase that has many cellular functions associated with a wide repertoire of substrates located in a variety of cellular compartments (Duncan et al., 2010; Litchfield, 2003; Pinna, 2002). Notably, a number of transcriptional factors are known to be phosphorylated by CK2. In fact, Meggio and Pinna (2003) reported that 60 of 307 putative substrates were transcriptional factors. Thus, the role of phosphorylation upon transcriptional factors by CK2 is an important issue. Nevertheless, the molecular basis, and mode of action, of transcriptional regulation by CK2 remains largely unknown because of the lack of structure-based evidence, and because of complexities associated with the promiscuity of CK2, although many observations concerning CK2 phosphorylation have been documented (Meggio and Pinna, 2003). This is in stark contrast to the more well-studied transcriptional factors, such as AP1, STAT, and SMADs, which are phosphorylated

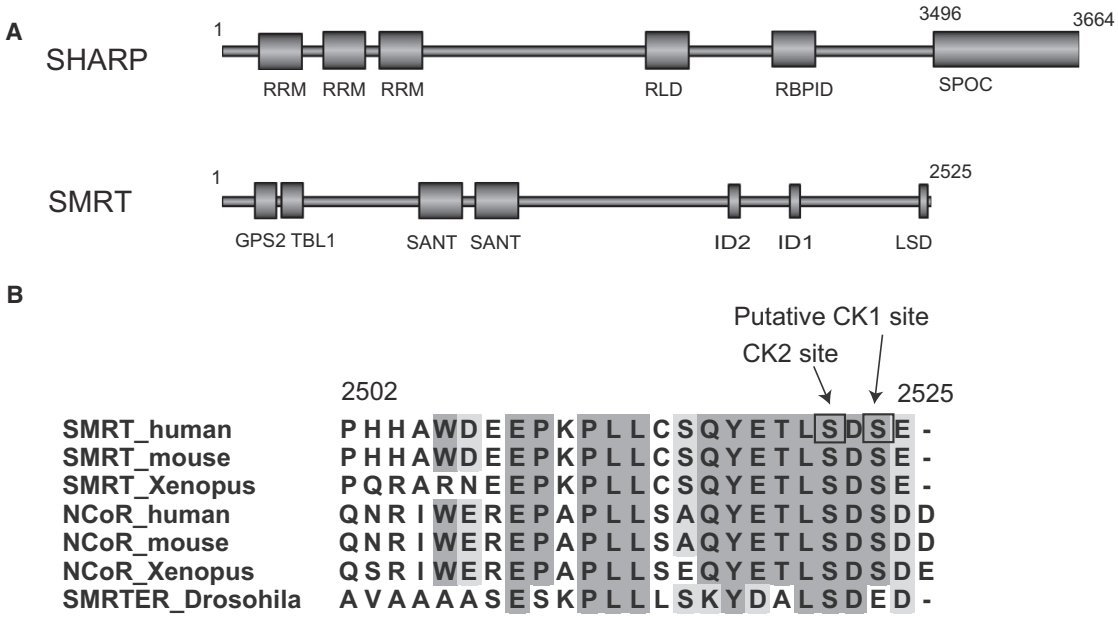

Figure 1. Schematic Representations of SHARP and SMRT

(A) Schematic representations of the domain structure of human SHARP and human SMRT. RRM (RNA recognition motif), RID (nuclear receptor interaction domain), RBPID (RBP interaction domain), and SPOC domains are indicated in SHARP, and GPS2- and TBL1-interacting regions, SANT-like domains, and ID and LSD motifs are indicated in SMRT.

(B) Sequence alignments of C-terminal regions of SMRT, NCoR, and SMRTER. The putative CK1 site (S/T-X-X-X-S) and CK2 site (S/T-X-X-E) are also indicated.

and regulated by their own specific kinases in signal transduction pathways (Darnell et al., 1994; Johnson and Lapadat, 2002; Kretzschmar and Massagué, 1998).

The crystal structure of the SPOC domain from SHARP has already been reported (Ariyoshi and Schwabe, 2003). However, the structure of the SPOC/SMRT complex has not yet been reported, and characterization of its molecular interaction has been elusive. Here, we demonstrate that the phosphorylation of SMRT by CK2 markedly enhances interaction with the SPOC domain of SHARP as a phosphorylation-recognizing domain. We present the structure determination of the SPOC domain of SHARP/phosphorylated SMRT peptide complex, as determined by nuclear magnetic resonance (NMR). We also present the molecular recognition mechanism of phosphorylated SMRT by SHARP, as revealed by structural analysis in conjunction with surface plasmon resonance (SPR) and reporter assays. We thus present a compelling structure-based example in which phosphorylation by CK2 regulates transcription.

RESULTS

The SPOC Domain of SHARP Preferentially Binds Phosphorylated SMRT

Although the C-terminal LSD motif of SMRT was suggested to be important for direct interaction with the SPOC domain (Figure 1A), the role of phosphorylation upon S2522 in the LSD motif has not been identified. Furthermore, a database search based on a CK1 phosphorylation consensus sequence (S/TXXX**S**) using the Scansite server (http://scansite.mit.edu/) showed that the S2524 adjacent to the LSD motif was a putative CK1 site (TLSD**S**E) (Figure 1B). Thus, we initially investigated the effects of phosphorylation using the recombinant SPOC domain (aa 3496–3664) and a 24-residue C-terminal SMRT peptide (aa 2502–2525). When the peptide was not phosphorylated, NMR titration experiment exhibited low affinity because the chemical shift changes of the SPOC domain signals upon unlabeled SMRT peptide binding demonstrated fast exchange, a feature that is typically observed in cases of weak binding (Figure 2A, left panel). In contrast, NMR titration experiments using the double phosphorylated peptide, in which both S2522 and S2524 (CK2 and putative CK1 site, respectively) were phosphorylated, showed binding in a slow exchange manner, which is typically observed in cases of stable binding (Figure 2A, right panel).

We next estimated the minimal length of phosphorylated SMRT required for interaction with the SPOC domain by comparison of NMR titration experiments using phosphorylated 24- (aa 2502–2525), 8- (aa 2518–2525), and 5- (aa 2521–2525) residue peptides (Figure 2B; Figure S1 available online). As a result, the 8-residue peptide showed an almost identical chemical shift perturbation pattern to that of the 24-residue peptide in slow exchange manner, although the magnitude of the chemical shift change was slightly smaller in the 8-residue experiment (Figures 2B and 2C). This indicates that the molecular recognition mechanism is essentially retained in the 8-residue peptide in comparison with the 24-residue peptide. However, the 5-residue peptide L(pS)D(pS)E showed only minor chemical shift perturbation (Figures 2B and S1), indicating that this peptide lost affinity despite including the LSD motif and phosphorylation. Thus, the LSD motif was not sufficient to bind to the SPOC domain even though it was phosphorylated. We found that additional N-terminal residues were required for interaction to take place.

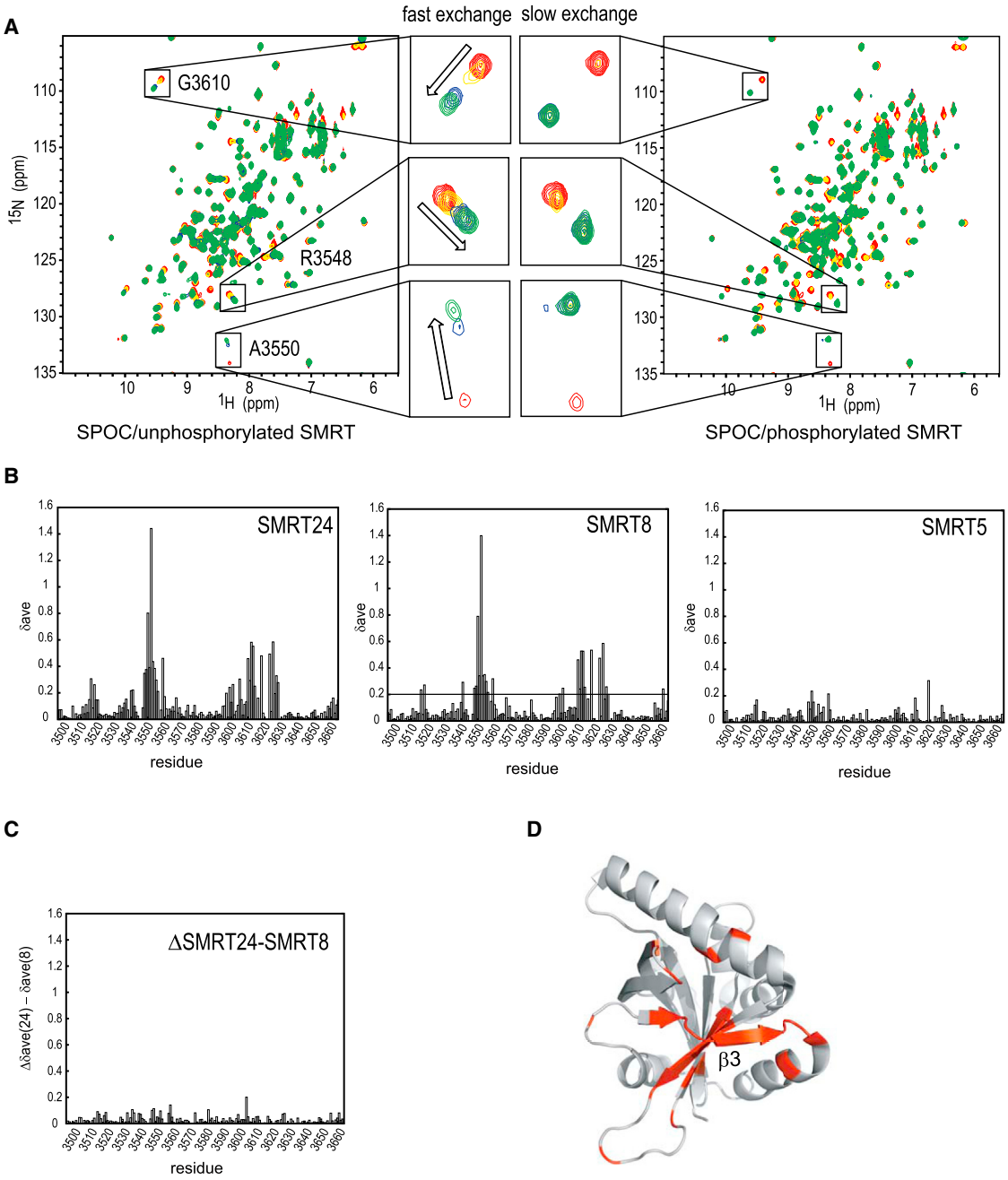

Figure 2. Binding of Phosphorylated SMRT to the SPOC Domain

(A) Chemical shift changes of the SPOC domain upon unphosphorylated 24-residue SMRT peptide binding (left) and doubly phosphorylated 24-residue SMRT peptide binding (right). The ^{1}H-^{15}N HSQC spectra with 1:0, 1:0.5, 1:1, and 1:2 molar ratios of ^{15}N-labeled SPOC domain and unlabeled SMRT peptide with/without phosphorylation are shown by red, yellow, blue, and green, respectively.

(B) Chemical shift changes of the SPOC domain upon 24-, 8-, and 5-residue peptide bindings are shown as weighted average shift difference values, δ_{ave}, calculated as $[\delta_{1H}{}^2 + 0.14(\delta_{15N})^2]^{1/2}$, where δ_{1H} and δ_{15N} represent the difference in ppm between the free and complex forms.

(C) Difference of the chemical shift changes between 24- and 8-residue peptides as shown in $\Delta\delta_{ave}$, where the $\Delta\delta_{ave} = \delta_{ave}(24) - \delta_{ave}(8)$.

(D) Mapping of the most-affected residues upon the ribbon model of the SPOC domain crystal structure (PDB ID code 1OW1). Residues with significant chemical shift changes (δave(8) larger than 0.2) in the titration experiment using an 8-residue peptide (at 1:1 molar ratio) are colored in red.

Structure Determination of SPOC/Phosphorylated SMRT Complex

To determine the SMRT interaction site on the SPOC domain, we analyzed chemical shift changes of the HSQC spectrum from the SPOC domain. We mapped residues whose chemical shift changed dramatically upon the peptide p-SMRT-C8 (aa 2518–2525, the C-terminal SMRT peptide double phosphorylated at S2522 and S2524) binding onto the crystal structure of the

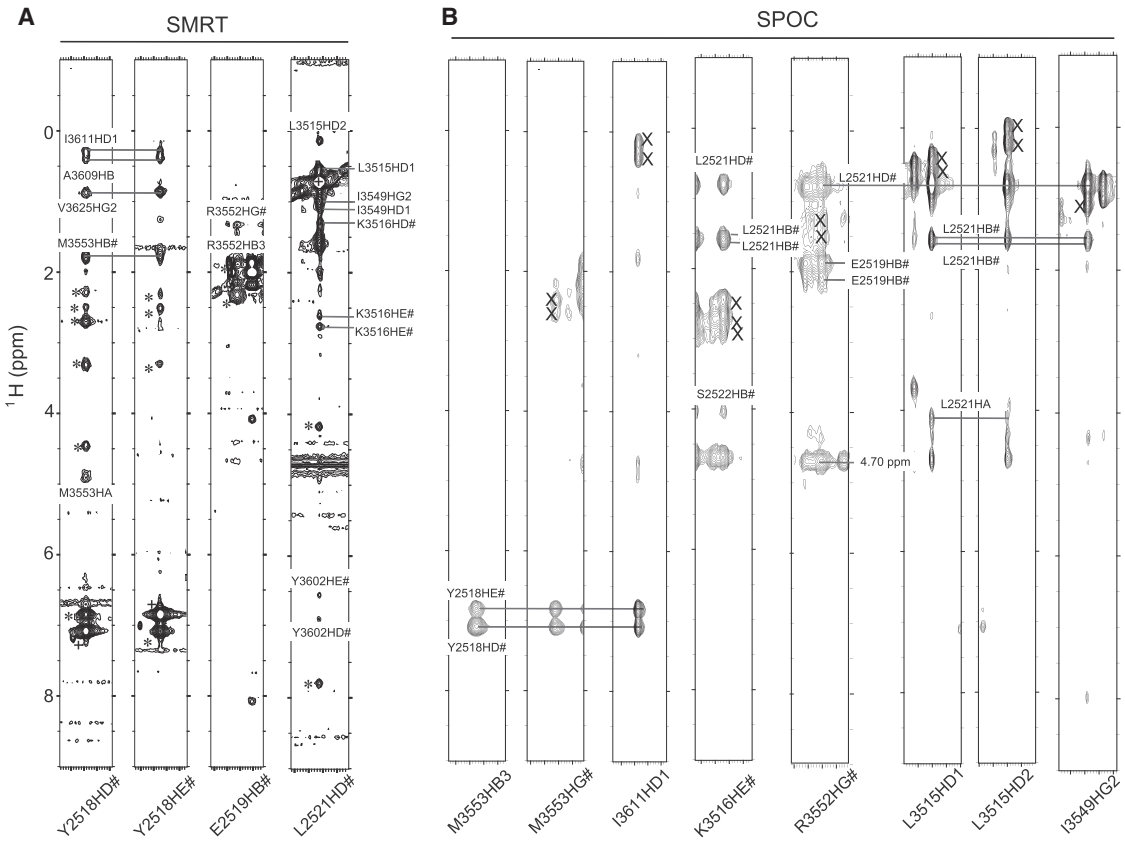

Figure 3. Intermolecular NOEs

(A) Selected regions of the 3D ^{13}C-edited NOESY spectrum of the complex formed between ^{13}C,^{15}N-labeled SMRT and the unlabeled SPOC domain. Intramolecular cross-peaks and diagonal peaks are shown in asterisk and cruciform, respectively.

(B) Selected regions of the 3D ^{13}C-edited (F_2)/^{13}C^1,^{5}N-filtered (F_1) NOESY HSQC spectrum of the complex formed between ^{13}C/^{15}N-labeled SPOC and unlabeled SMRT. Incompletely suppressed peaks are indicated by an X.

SMRT-free SPOC domain (Protein Data Bank [PDB] ID code 1OW1). Interestingly, the perturbed residues were confined to a region around the strand β3 (around residue 3552) of the SPOC domain (Figures 2B and 2D). Ariyoshi and Schwabe (2003) previously described the interaction surface as deduced from the inspection of crystal packing and mutagenesis. At the N-terminal of the crystallized form, six residues stretched from another molecule attached to the β3 strand (Figure S2A). Previous studies have proposed that the surface surrounding β3 represents the peptide binding region (Ariyoshi and Schwabe, 2003). The binding region we identified was almost identical to that described in this previous report, although there was a remarkable difference in the peptides used, specifically in the sense that our peptide was phosphorylated, while that used in the previous study was not.

We next determined the solution structure of the SPOC/p-SMRT-C8 complex using heteronuclear NMR to reveal how phosphorylation contributes to interaction. The use of chemically synthesized and partially labeled SMRT peptide facilitated the NMR assignment process (Mikami et al., 2013). Together with the two-dimensional (2D) ^{13}C, ^{15}N-filtered (F2) TOCSY experiment, we could assign ^{1}H chemical shifts in an unlabeled part of the SMRT peptide, such as Hβ, Hα, and amide H of pS2522.

NMR spectra used to monitor inter/intramolecular ^{1}H-^{1}H nuclear Overhauser effects (NOEs) were of adequate quality in order to pursue structural determination of the complex. In particular, Y2518 and L2521 of the labeled peptide provided well-dispersed and unambiguous intermolecular NOEs from the three-dimensional (3D) ^{13}C-edited NOESY HSQC experiment using an unlabeled SPOC domain/^{13}C, ^{15}N DELY-labeled p-SMRT-C8 complex at an initial stage of manual identification of intermolecular NOEs (Figure 3A). In addition to manually assigned NOE cross-peaks, the inter- and intramolecular NOE cross-peaks observed in the NOESY spectra were assigned by using an automatic-iterative manner. Finally, intermolecular NOEs were confirmed manually by a 3D ^{13}C-edited (F_2)/^{13}C^1,^{5}N-filtered (F_1) NOESY HSQC experiment using a ^{13}C,^{15}N-labeled SPOC domain/unlabeled p-SMRT-C8 complex (Figure 3B). In total, the solution structure of the SPOC/p-SMRT-C8 complex was determined from over 4,000 NMR-derived distance restraints, including 97 intermolecular distance restraints (Table 1).

The ensemble of 20 structures was in excellent agreement with a large body of well-defined experimental data (Figure 4A; Table 1). The root-mean-square deviations (rmsds) of the backbone and all heavy atoms of SPOC/p-SMRT-C8 complex were 0.38 and 0.82 Å, respectively, except for disordered regions. Bound

Table 1. NMR Structure Determination Statistics for the SPOC/p-SMRT-C8 Complex

	SA	$SA_{water\ refined}$
Total number of distance constraints	4,047	
Intraresidue	754	
Short range (|i − j| = 1)	973	
Middle range (|i − j| = 2,3,4)	674	
Long range (|i − j| > 4)	1,549	
Intermolecular	97	
Hydrogen bond constraints	94 × 2	
Dihedral Constraints		
ϕ, φ, χ_1	129, 131, 40	
Rmsds from experimental constraints[a]		
Distance (Å)	0.0214 ± 0.0003	0.027 ± 0.001
Angle (°)	0.491 ± 0.06	0.79 ± 0.05
Rmsds from idealized covalent geometry		
Bonds (Å)	0.00141 ± 2 × 10^{-5}	0.00423 ± 7 × 10^{-5}
Angles (°)	0.318 ± 0.002	0.557 ± 0.009
Impropers (°)	0.206 ± 0.003	1.59 ± 0.07
PROCHECK Ramachandran plot[b]		
Residues in most-favored regions (%)	85.5	89.5
Residues in additionally allowed regions (%)	12.9	9.0
Residues in generously allowed regions (%)	0.2	0.6
Residues in disallowed regions (%)	1.4	0.9
Average atomic rmsds from the average structure		
Backbone (Å)	0.30	0.38
All heavy (Å)	0.74	0.82

These statistics comprise the lowest energy ensemble of the 20 structures obtained from 100 starting structures. Structure calculations were performed using CNS (v. 1.2).
[a]None of these structures exhibited distance violations >0.5 Å or dihedral angle violations >5°.
[b]Evaluated for the SPOC domain residues 3496–3540, 3546–3616, and 3624–3664 and the SMRT residues 2518–2522.

p-SMRT-C8 adopts an extended structure, the orientation of the side chains of Y2518, E2519, L2521, and pS2522 are well defined, supported by intermolecular NOEs. Of note, the 4.70 ppm intermolecular NOE observed from R3552Hγ was probably due to hydrating water (Figure 3B), although the water(s) was not implemented in the structure calculation. The last C-terminal three residues, YETL(pS)***D(pS)E***, were not well defined in the complex structure, implying that these residues are flexible, even in complex (Figure 4A). In fact, {^{1}H}-^{15}N heteronuclear NOE values of D2523 and E2525 were negative, indicating flexibility of the C-terminal region in the complex state (Figure 4B).

Overall Structure of the Complex

The mainframe of the SPOC domain structure in complex with p-SMRT-C8 was identical to that of the free SPOC structure composed of a seven stranded antiparallel β sheet and six α helices (Figure 4C). Interaction between the SPOC domain and p-SMRT-C8 did not cause significant structural changes to the SPOC domain. The atomic rms difference between the SPOC domain in complex with the p-SMRT-C8 peptide and free SPOC was 1.3 Å when backbone N, Cα, and C' atoms of the well-defined parts were superimposed.

As expected from our chemical shift perturbation experiments, p-SMRT-C8 was bound to a hydrophobic shallow cleft that was rich in basic residues at the rim (Figure 4D). p-SMRT-C8 associates with SPOC in 1:1 stoichiometry and orientation of the peptide relative to the SPOC domain is well defined, consistent with the large number of NMR restraints (Figures 4A and 4C; Table 1). The buried solvent-accessible area of the SPOC/p-SMRT-C8 interface extends over 1,230 Å^2, including various types of noncovalent interactions. The shallow hydrophobic cleft decorated by basic charges on the SPOC domain is occupied by the side chain of L2521 from the LSD motif of SMRT as a lid (Figure 4D).

Molecular Recognition of Phosphorylated SMRT by the SPOC Domain

p-SMRT-C8 (YETL(pS)D(pS)E) is recognized by numerous intermolecular interactions by the SPOC domain. As described above, our NMR titration showed that the N-terminal part (Y2518, E2519, and T2520) is required for binding. In the complex, the first residue (Y2518) forms hydrophobic interactions with the hydrophobic side chains of M3553 and I3611 via its aromatic ring (Figure 4E). The E2519 side chain potentially interacts with R3552 and R3554 via electrostatic interactions or hydrogen bonding (Figure 4E). The side chain of T2520 is exposed to the opposite side of the complex interface and is therefore unlikely to play an important role in complex formation. A possible hydrogen bond donor to the T2520 hydroxyl group is the side chain of Q3551 on strand β3 (Figure 4E).

Leu2521, the first residue of the LSD motif, adjacent to the site of CK2 phosphorylation, is docked into the small hydrophobic cleft of the SPOC domain formed by strand β3 and the side chain of I3549 and L3515 (Figure 4E). A striking feature of SPOC/SMRT interaction is molecular recognition of the phosphate on pS2522 (CK2 site) by the SPOC domain. The phosphate group of pS2522 is located on the edge of a shallow cleft. Although a lack of NMR distance information restricted interpretation of the structure, and because phosphate does not provide NOEs, the orientation of the side chain of pS2522 was defined by intermolecular NOEs between side chain of K3516 and Hβ of pS2522. It appears that R3552, located close to the phosphate group of pS2522, is an attractive candidate as a residue critical to hydrogen bond formation to the phosphate (Figure 4E). In addition, positive charges of the side chain of two closely located lysines (K3516 and K3606) potentially contribute to binding via electrostatic interactions or hydrogen bonding with the phosphate.

Notably, Y3602 also closely locates to the phosphate and possibly contributes to the proper orientation of the side chains of these two lysines (K3516 and K3606). The aliphatic side chains of the lysines are located close to the side chain of Y3602 (Figure 4E). Those of the δCH2 signals of K3516 and K3606 showed

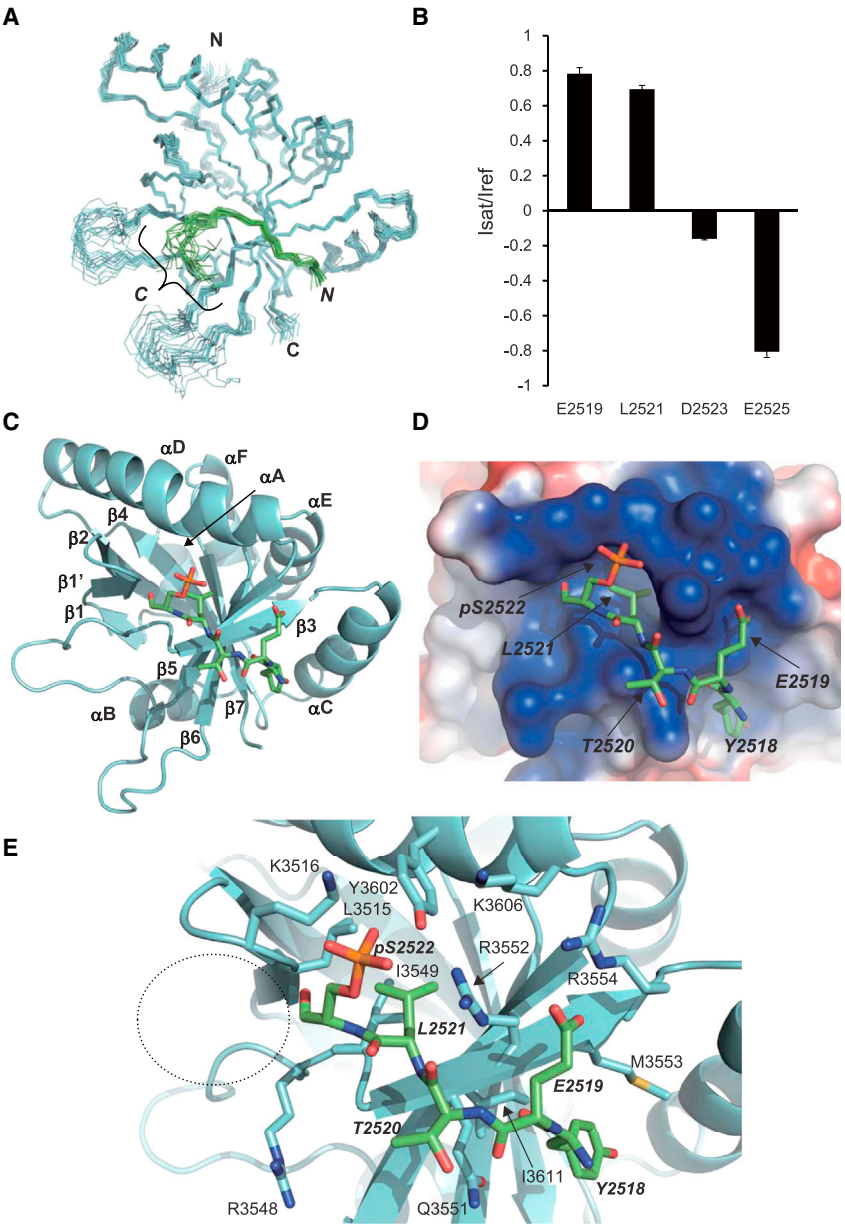

Figure 4. Structure of the SPOC/p-SMRT-C8 Complex

(A) A best-fit superimposition of the final 20 simulated annealing structures of the SPOC/p-SMRT-C8 with the lowest energies as determined by NMR. The SPOC domain and SMRT peptide backbone are colored cyan and green, respectively.

(B) {^{1}H}-^{15}N NOE values of synthesis DELY selective ^{13}C,^{15}N-labeled phosphorylated SMRT peptide in complex with SPOC domain.

(C) The SPOC domain and SMRT peptide are depicted by ribbon model and stick representation, respectively, using the same color and molecular orientation as in (A).

(D) Electrostatic potential of the SMRT binding site of the SPOC domain. Molecular orientation of the image is identical to (A). The surface is covered by electrostatic potential, where the potential is colored and ranges from −2 kT/e in red to +2 kT/e in blue.

(E) Close-up view of the SMRT binding site of the SPOC domain. The side chains of the SPOC domain residues, which contribute to interaction with SMRT, are shown and labeled. The residues of SMRT peptide are labeled in italics. The site in which three residues are disordered within the C-terminal of SMRT is depicted by a dotted circle. Molecular orientation is the same as in (A).

upfield shifts, 1.03 and 1.16 ppm respectively, probably due to ring current shift caused by Y3602.

The last three C-terminal residues of p-SMRT-C8, D2523, pS2524, and E2525 were mobile in the complex as shown in Figures 4A and 4B. Notably, however, the negatively charged side chains of these residues potentially form electrostatic interactions with R3548 located close by (Figure 4E).

Comparison between the crystal packing and SPOC/p-SMRT-C8 complex structure revealed how crystal packing interaction mimics phosphorylated SMRT peptide recognition. The hydrophobic interactions mediated by Y2518 and L2521 of the SMRT peptide are replaced by the hydrophobic interactions mediated by V3496 and V3499, respectively, in the crystal packing (Figures S2A and S2B). In addition, the electrostatic interaction mediated by E2519 of SMRT is replaced by the interaction mediated by D3497. Of note, instead of the phosphate, the backbone carbonyl of V3499 locates to a very similar position in the crystal packing (Figures S2A and S2B).

SPR Analyses

NMR titration experiments using unphosphorylated and phosphorylated peptides clearly showed that the SPOC domain preferentially binds the phosphorylated peptide as described. Furthermore, we performed SPR analyses using the purified wild-type SPOC domain and chemically synthesized SMRT peptide with various phosphorylation patterns in order to quantify differences in affinity. As expected, the K_D value of double phosphorylated peptide was significantly lower (approximately 100 times) than that of unphosphorylated peptide. K_D values for double phosphorylated and unphosphorylated peptides were $7.4 \pm 2.4 \times 10^{-7}$ M and $5.4 \pm 5.6 \times 10^{-5}$ M (Figures 5A and 5B), respectively. Using isothermal titration calorimetry (ITC), this increased affinity was confirmed in solution state, and the obtained K_D was almost consistent with SPR: $1.9 \pm 1.8 \times 10^{-7}$ M for doubly phosphorylated peptide (Figure 5C). Furthermore, the K_D value of the CK2 single site phosphorylated peptide obtained from SPR was $7.3 \pm 2.9 \times 10^{-7}$ M, comparable to that of the double phosphorylated peptide (Figures 5A and 5B). In contrast, the single site phosphorylation of S2524 (putative CK1 site) showed a marginal effect upon binding, and K_D was determined as $3.1 \pm 1.4 \times 10^{-6}$ M (Figures 5A and 5B). These data indicate that phosphorylation of the CK2 site is of critical importance for

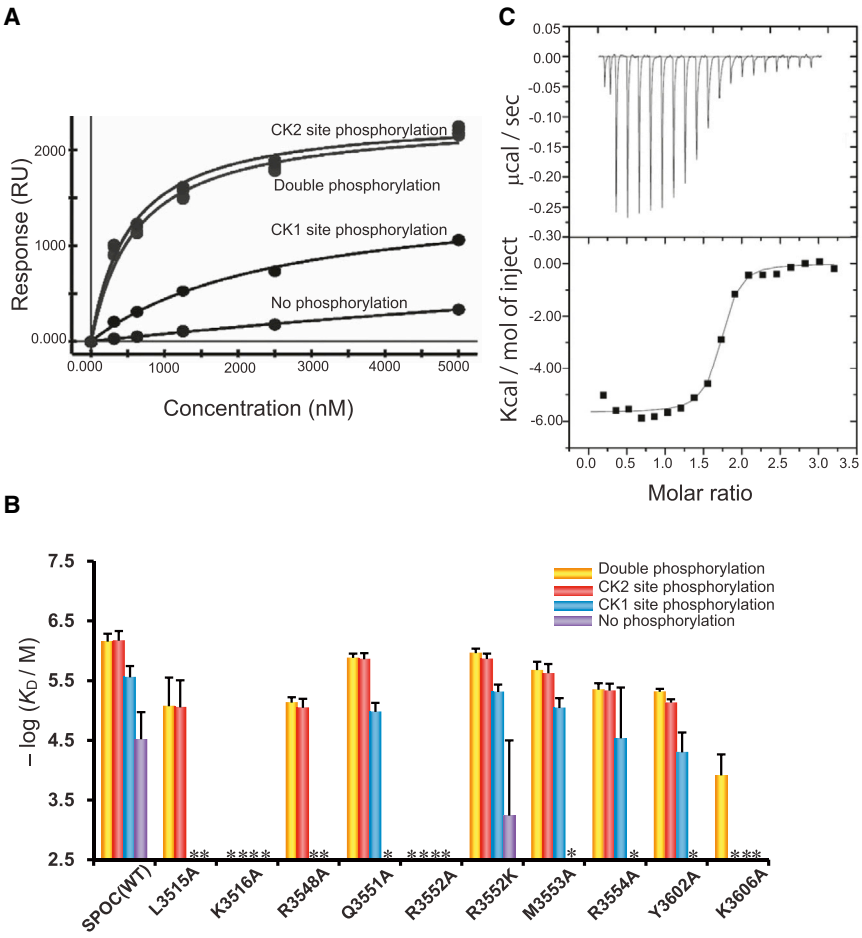

Figure 5. In Vitro Binding Assay

(A) Equilibrium SPR analysis for the wild-type SPOC domain with 24-residue SMRT peptides (W/WO phosphorylation). The 24-residue peptides were immobilized to the sensor chip.

(B) SPR analyses of mutants and the wild-type SPOC domain with SMRT peptides. The yellow, red, blue, and purple bars indicate affinities shown as values of $-\log(K_D/M)$ for SMRT peptides with double phosphorylation, phosphorylation of the S2522(CK2 site), phosphorylation of the S2525(CK1 site), and nonphosphorylation, respectively. To use a dimensionless number in log, K_D was divided by M. The asterisk represents $-\log(K_D/M)$ value <2.5, and the affinity was too low to obtain accurate values by rigorous analysis. The error bars represent SD from at least three independent measurements.

(C) The top panel shows an ITC thermogram for binding of the wild-type SPOC domain to p-SMRT-C8. The bottom panel shows the integrated heat of each injection after correcting for the heat produced by diluting the SPOC domain.

SPOC/SMRT interaction, whereas phosphorylation of the CK1 site is of little importance.

We next carried out site-directed mutagenesis experiments in order to assess the individual contribution of interfacial residues of the SPOC domain toward the overall stability of the SPOC/SMRT complex. To exclude the mutant, which was devoid of appropriate folding, we accessed the tertiary structure of each mutant by measuring NMR spectra (Figure S3). As a result, we confirmed the structural integrity of all mutants, except for I3549A and I3611A, which we were unable to express and purify.

As expected, Ala substitution of R3552, a key candidate residue for pS2522 recognition, exhibited a dramatic reduction in affinity (Figure 5B). To be noticed, affinities for all peptides were significantly reduced. This implies that R3552 contributes to interaction not only with the phosphate but also with other acidic component, probably E2519, by electrostatic interactions (Figure 4E). Interestingly, mutation of R3552 to Lys, which retains basic charge, exhibited slight reduction of binding affinity but retained tendency for differing affinities for various phosphorylation patterns on the SMRT peptide (Figure 5B). K3516A and K3606A also exhibited greatly diminished binding for the CK2 phosphorylated SMRT peptide, consistent with the determined structure. Furthermore, these residues also exhibit significantly reduced affinities for other SMRT peptides similar to the case of R3552A, implying that they also interact with an acidic part other than the phosphate by long-range electrostatic interaction (Figure 5B).

Notably, R3548A lost affinity in a remarkable manner specifically to single phosphorylated (CK1 site) SMRT compared to the wild-type (Figure 5B). In the determined structure, R3548 was located in the vicinity of the phosphate at the CK1 site, although the structure is not converged and flexible (Figures 4A and 4E). This significant reduction may reflect the loss of electrostatic interaction between R3548 and the CK1 site phosphate in vitro.

As a hydrophobic residue, L3515A showed reduction in affinity (Figure 5B). I3549 and I3611 also contribute to intermolecular interaction, judging from the determined structure. Nevertheless, we were not able to produce I3549A and I3611A mutants as they were formed within an inclusion body, and we could not therefore investigate their contribution to complex formation. However, this implies that such mutants lack the structural integrity of the SPOC domain. Thus, I3549 and I3611 probably play an important role in maintaining structure of the SPOC domain in addition to stabilizing the complex. M3553A also showed a slight reduction in affinity (Figure 5B).

As described, Y3602 contributes to the appropriate orientation of the side chains of the two lysines K3516 and K3606. As expected, mutation of Y3602 to Ala, which lacks the aromatic side chain, caused reduction in affinity (Figure 5B). Mutation of Q3551, a potential hydrogen bond acceptor against T2520, showed only marginal effect (Figure 5B).

Repression Analyses

The structural basis obtained from the SPOC/p-SMRT-C8 complex structure in conjunction with SPR analysis was also tested in living cells. Effects of SPOC domain mutations upon transcription were analyzed by luciferase reporter assay using cultured

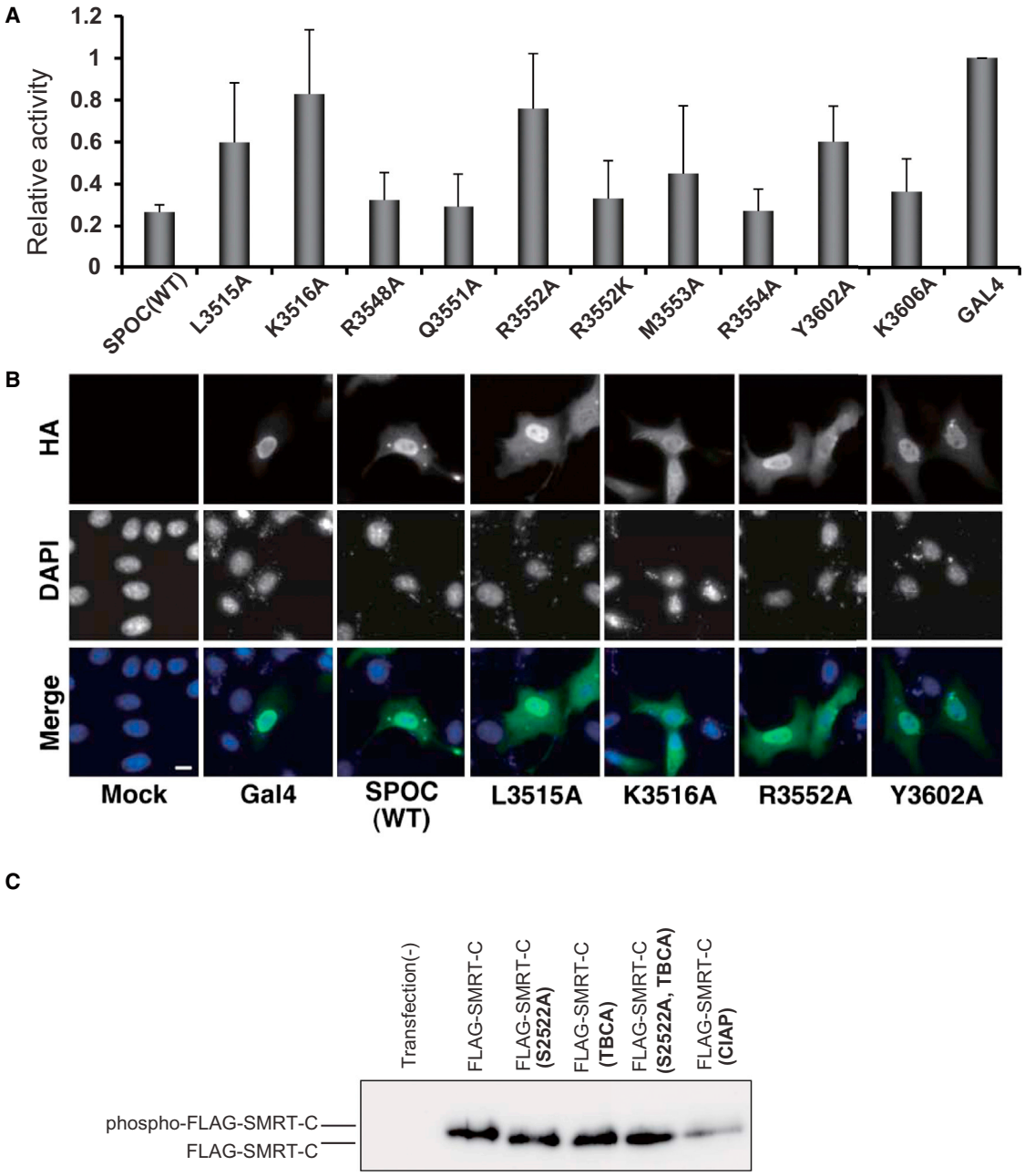

Figure 6. Significance of Phosphorylation in Cell-Based Assays

(A) Relative activities of the luciferase reporter as determined by firefly luciferase units normalized to Renilla luciferase. All data represent mean values of three independent experiments, and error bars represent SD. The error bars represent SD from at least three independent measurements.

(B) Intracellular localization of wild-type and mutants of HA-tagged GAL4-SPOC visualized by immunofluorescence. Scale bar represents 10 μm.

(C) Alteration in the electrophoretic mobility of SMRT. pFLAG-SMRT-C and pFLAG-SMRT-C (S2522A) were introduced into CV-1 cells. Whole-cell lysates were resolved by SDS-PAGE and visualized by immunoblotting using an antibody specific for the FLAG tag. The lane labeled with TBCA represents the sample treated with the CK2 inhibitor tetrabromocinnamic acid (TBCA) during cell culture, whereas the lane labeled with CIAP represents the sample treated with calf intestinal alkaline phosphatase (CIAP) prior to SDS-PAGE and immunoblotting.

CV-1 cells. An expression vector for the SPOC domain fused to the GAL4 DNA-binding domain (Gal4DBD-SPOC) and a GAL4-responsive luciferase reporter vector were transfected, and luciferase activities were measured. We confirmed that similar levels of HA-tagged GAL4DBD-SPOC mutant proteins were expressed in the transfected cells under the same condition of repression assay (Figure S4). As seen in SPR analyses, mutations of the key residues for molecular recognition of phosphorylation at the CK2 site, K3516A and R3552A, impaired the repression activity of GAL4DBD-SPOC, and reporter activities were recovered to a level similar to the Gal4DBD-only plasmid (Figure 6A). Meanwhile, mutation of L3515, which contributes to the complex

formation by hydrophobic interaction with L2515 of SMRT, impaired repression in a moderate manner (Figure 6A). Mutation of Y3602, which contributes to the appropriate side-chain conformations of K3516 and K3606, also moderately impaired repression (Figure 6A). Interestingly, mutation of R3548 in the vicinity of the phosphate group of the CK1 site in the determined structure (Figure 4E) exhibited almost no effect upon repression (Figure 6A). Thus, the significance of phosphorylation at the CK1 site was not evident in cultured cells. We also confirmed intracellular localization patterns of the mutants by immunofluorescence (Figures 6B and S5). All mutants tested, including the mutants K3516A and R3552, which impaired repression activity, localized appropriately to the nucleus as with the wild-type, indicating that mutations do not affect localization of the SPOC domain (Figure 6B).

Phosphorylation on S2522

To characterize the phosphorylation of S2522 by CK2 in CV-1 cells, we monitored alteration in the electrophoretic mobility of SMRT with and without treatment with the specific CK2 inhibitor, tetrabromocinnamic acid (TBCA). Prior to the phosphorylation experiment using CV-1, we confirmed the direct phosphorylation on S2522 by CK2 in vitro, using the purified GST-fused SMRT peptide (YETLSDSE), GST-SMRT-C8. We detected the incorporation of ^{32}P using $^{32}P(\gamma)$-ATP for the GST-SMRT-C8 and that this incorporation was abolished in the S2522A mutant GST-SMRT-C8 (S2522A) (Figure S6). The inhibitor TBCA suppressed such incorporation very effectively (Figure S6). These studies indicate that the S2522 is the site of phosphorylation by CK2. These results are consistent with the in vitro experiment previously reported (Zhou et al., 2001).

Next, the C-terminal part of SMRT (aa 2321–2525) fused to a FLAG tag, and its S2522A mutant, FLAG-SMRT-C and FALG-SMRT-C (S2522A), were expressed in CV-1 cells. Cells were harvested and lysed, and whole-cell lysates were resolved by SDS-PAGE and immunoblotting. FALG-SMRT-C showed a delay in electrophoretic mobility against FALG-SMRT-C (S2522A). Furthermore, treatment of FALG-SMRT-C with alkaline phosphatase recovered mobility, indicating that FALG-SMRT-C was phosphorylated at S2522 in CV-1 cells (Figure 6C). Notably, FALG-SMRT-C expressed in the presence of TBCA did not exhibit a delay in electrophoretic mobility (Figure 6C). Thus, it could be concluded that the responsible kinase for S2522 is CK2.

DISCUSSION

SPR analysis showed that single site phosphorylation on SMRT by CK2 makes a significant contribution to binding affinity to the SPOC domain. This is in stark contrast to the moderate effect of phosphorylation upon the adjacent CK1 site (Figures 5A and 5B). Paradoxically, Ala substitution of R3548 within the SPOC domain, which is in the vicinity of the CK1 site phosphate in the complex, showed loss of affinity for the single phosphorylated (CK1) SMRT peptide in SPR experiments, although reporter assays using CV-1 cells showed no effect for R3548A. In contrast, remarkable effects for the Ala substitutions of R3552 and K3516 within the SPOC domain, which were located close to the CK2 site in the complex, were evident in both SPR and reporter analyses. Collectively, these results suggest that the SPOC domain, in terms of a molecule, is responsible mainly for the molecular recognition of CK2 site phosphorylation and can also recognize CK1 site phosphorylation. However, it is possible that phosphorylation of the CK1 site of SMRT does not occur in cells during the repression assay. In fact, a phosphor-proteomic approach recently surveyed widespread protein phosphorylation and determined that the CK2 site of SMRT was phosphorylated, whereas CK1was not (Olsen et al., 2006). As a consequence, mutation of R3548, which is responsible for CK1 site recognition, showed no effect, whereas mutations of R3552 and K3516, key residues for CK2 site recognition, showed significant effects. In other words, the possibility of phosphorylation upon the CK1 site, or double phosphorylation events upon SMRT in cells under specific conditions, has yet to be tested and should be investigated in order to promote our understanding of this important mechanism.

As key residues of SMRT for SPOC domain binding, NMR binding analyses suggested that the N-terminal three residues, Y2518, E2519, and T2520, are also required for binding in addition to the LSD motif and phosphorylation. Inspection of the complex structure showed that Y2518 and E2519 are recognized by SPOC domain residues, whereas T2520 is exposed to the solvent (Figure 4E). Also, alanine substitution of Q3551, a putative counterpart for T2520, showed subtle effects in SPR analysis and reporter assays (Figures 5B and 6B). It is probable that the T2520 residue existing between the N-terminal YE and LSD motifs is not important for interaction but may play a role as a spacer or linker. In fact, preliminary SPR analysis showed that alanine mutations of Y2518 and E2519 resulted in loss of affinity, whereas glycine mutation of T2520 retained affinity for the SPOC domain (Figure S7). Collectively, these data might suggest that YExL(pS)D could represent a possible core sequence for SPOC domain binding.

We next contemplated the biological significance of CK2 phosphorylation. CK2 is known to localize to the nucleus, cytoplasm, and plasma membrane and phosphorylates many proteins as this promiscuous kinase targets a wide variety of substrates (Litchfield, 2003; Pinna, 2002). In general, CK2 activity is closely related to cell state, such as viability, cell growth, proliferation, the cell cycle, and cell survival (Cabrejos et al., 2004; Duncan et al., 2010; Homma et al., 2002, 2005; Johnston et al., 2002; Lin et al., 2006; Litchfield, 2003; Panova et al., 2006; Pinna, 2002). It is thus interesting to speculate that CK2 phosphorylation of SMRT plays a role in crosslinking between the transcriptional repression by SHARP and cell state. Phosphorylation on SMRT by CK2 may represent a "flag" providing information concerning cell state and suggesting that the SPOC domain may be a decoder. SHARP is known as an inducible cofactor in hormone response and is able to repress SRA-mediated transactivation by glucocorticoid receptor and estrogen receptor in an autoregulatory manner (Shi et al., 2001). Presumably, the phosphorylation by CK2 contributes to the fine-tuning of hormonal response. Future OMICS studies for target genes regulated by SHARP are now required in order to advance our understanding of the regulatory mechanisms involved. Of particular note is the fact that DEK, a coactivator for the nuclear receptor ecdysone receptor, is also phosphorylated by CK2 in *Drosophila*, and such phosphorylation is prerequisite for DEK

activity (Sawatsubashi et al., 2010). This also suggests that CK2 has an indispensable role in the precise regulation of hormone response.

Throughout the cell cycle, SMRT and NCoR are known to locate predominantly to the nucleus (Espinosa et al., 2002). Consequently, phosphorylation is unlikely to exert effect upon the intracellular localization of SMRT in clear contrast to the well-studied STAT and SMADs (Darnell et al., 1994; Kretzschmar and Massagué, 1998), which translocate from cytosol to nucleus in response to specific phosphorylation. Rather, phosphorylation of SMRT by CK2 could be regarded as being a molecular switch for the SPOC domain binding in the nucleus. In contrast, it has been reported that MAPKs, MEK-1 and MEKK-1, phosphorylate SMRT, resulting in inhibition of repressive function and perturbation in localization (Hong and Privalsky, 2000).

In addition, a recent SMRT/HDAC3 crystallographic study showed that IP4 bound to the interface of SMRT/HDAC3, suggesting an unknown regulation by IP4 (Watson et al., 2012b). Interestingly, mice exhibiting point mutations at the interface in both NCoR and SMRT lost HDAC3 activity in vivo (You et al., 2013). It is noteworthy that we suggest an as-yet-unrecognized, multilayered regulatory network that links transcription and other cellular events by phosphorylation and that involves other post-translational modifications and unknown ligands.

Apart from the SPOC domain, there are several domains known to act as phosphorylated Ser binding modules, such as MSH2, WD40, WW, BRCT, and CID domains, and 14-3-3 proteins (Glover et al., 2004; Hao et al., 2007; Kubicek et al., 2012; Meinhart and Cramer, 2004; Yaffe and Smerdon, 2001). Our current experiment clearly showed that the SPOC domain recognizes CK2 site phosphorylation on SMRT by a specific interaction, such as K3516 and R3552 with the phosphate. We thus suggest that the SPOC domain is a phosphorylated Ser binding module, in addition to the already known ones.

We are also able to contemplate the diversity in structure and function of the SPOC domain that has been distributed among many proteins during evolution. Recently, the structure of the ACID domain of Med25, a mediator component of the coactivator complex, which binds the transcriptional activation domain (TAD) of VP16, has been characterized (Milbradt et al., 2011; Vojnic et al., 2011). Literatures describe the site of interaction for VP16 TAD within the ACID domain. Unexpectedly, the overall structure of the ACID domain is reported to be similar to the SPOC domain (Milbradt et al., 2011; Vojnic et al., 2011). Remarkably, the location of the VP16 binding site is similar to the SMRT binding site within the SPOC domain (Milbradt et al., 2011; Vojnic et al., 2011). It is attractive to speculate that this architecture may be widely used as a protein-protein interaction module in different systems.

EXPERIMENTAL PROCEDURES

Sample Preparation

The recombinant SPOC domain (aa 3496–3664) of human SHARP was expressed and purified as described previously (Mikami et al., 2013). Briefly, proteins were expressed in *Escherichia coli* strain BL21 Rosetta (DE3) (Novagen) as a fusion protein with glutathione S-transferase (GST). After the culture had reached an OD_{660} value of 0.5, isopropyl-l-thio-β-D-galactopyranoside (IPTG) was added to a final concentration of 1.0 mM to induce protein expression. The culture was incubated overnight at 20°C. The harvested cells were suspended in buffer containing 50 mM Tris-HCl (pH 8.0), 400 mM KCl, 1 mM dithiothreitol (DTT), 0.1 mM EDTA, and 20% glycerol and were lysed by sonication under ice-cold conditions. The cell lysate was centrifuged, and the supernatant was loaded onto a DEAE Sepharose Fast Flow (GE Healthcare), followed by a Glutathione Sepharose 4B (GE Healthcare) and was eluted by 30 mM reduced glutathione. The N-terminal GST-tag was cleaved using HRV3C proteinase. The target protein was purified by gel filtration (HiLoad 26/60 Superdex 75 pg, GE Healthcare) with buffer containing 30 mM HEPES (pH 7.5), 150 mM KCl, 1 mM DTT, and 0.1 mM EDTA.

The mutant SPOC domain expression vectors were created by inverted PCR. Following amplification of the vectors by inverted PCR using mutated primers, the template was digested by *DpnI*. Introduction of the desired mutation was confirmed by DNA sequencing. Mutant proteins were expressed and purified in the same manner as the wild-type.

NMR Spectroscopy and Structure Calculation

NMR experiments were performed at 30°C on a Bruker AVANCE 600 instrument equipped with a TXI CRYOPROBE and a Bruker AVANCE 900 instrument equipped with a TXI CRYOPROBE. For structure determination, the recombinant SPOC domain (aa 3496–3664) of human SHARP was used. The 8-residue phosphorylated SMRT peptide p-SMRT-C8 (YETL(pS)D(pS)E), corresponding to aa 2518–2525 of human SMRT, derived by solid-phase synthesis, was purchased from TORAY Research Center. Commercially available ^{13}C- and ^{15}N-uniformly labeled F-MOC amino acid precursors (aspartic acid, glutamic acid, leucine, and tyrosine [CIL]) were used for peptide synthesis and were able to obtain DELY-selective $^{13}C/^{15}N$-labeled phosphorylated peptide (Mikami et al., 2013). The solution structure of the SPOC/p-SMRT-C8 complex was determined using 0.9 mM complex solution in a buffer comprising 30 mM HEPES (pH 7.5), 1 mM DTT, and 0.1 mM EDTA with 93% H_2O/7% ^2H_2O or 99.9% ^2H_2O.

The sequential backbone resonance assignments in the complex were obtained from four triple-resonance experiments: 3D HNCO, 3D HN(CA)CO, 3D CBCA(CO)NH, and 3D HNCACB. The side-chain resonance assignments were obtained from five spectra: 3D C(CO)NH, 3D HC(CO)NH, 3D HCCH-TOCSY, 4D HC(CO)NH, and ^1H-^{13}C CT HSQC. The methyl resonances in 35/38 isopropyl groups of leucine and valine residues and 41/114 β-methylene groups were assigned in a stereospecific manner as previously reported (Mikami et al., 2013). The unlabeled part of the SMRT peptide was assigned by a 2D $^{13}C,^{15}N$-filtered (F2) TOCSY experiment using $^{13}C,^{15}N$-labeled SPOC domain/unlabeled p-SMRT-C8 complex sample.

The distance restraints derived by intramolecular NOEs were obtained from 3D ^{15}N-edited NOESY HSQC and 3D ^{13}C-edited NOESY HSQC with a mixing time of 100 ms. Intermolecular distance restraints were confirmed by a 3D ^{13}C-edited (F_2)/$^{13}C^1,^5N$-filtered (F_1) NOESY HSQC spectrum using $^{13}C,^{15}N$-labeled SPOC domain/unlabeled phosphorylated SMRT peptide sample. Dihedral φ and ψ angles derived from TALOS+ were also utilized (Shen et al., 2009). The 40 χ1 rotamers of the side chains were estimated from HNHB and HN(CO)HB experiments (Archer et al., 1991; Grzesiek et al., 1992).

The program CYANA (v. 3.0) was used with the CANDID protocol for structural restraint collection (Herrmann et al., 2002). The CYANA library file of the phosphorylated serine created by Craft and Legge (2005) was utilized. The ensemble of 100 SPOC/p-SMRT structures was calculated using the CNS program (v. 1.2) using a standard simulated annealing protocol (Brünger et al., 1998). Finally, structures were refined using a water refinement protocol (Linge et al., 2003). To take account of intermolecular interaction, a loose 5 Å upper bound was also used (R3552Nη,Hη-S2522PO, K3516Nζ-S2522PO K3606Nζ-S2522PO, and R3554Nζ,Nε-E2519Oε).

The final 20 ensemble structures with the lowest energy were checked by MOLMOL (Koradi et al., 1996), PROCHECK-NMR (Laskowski et al., 1996), and MolProbity (Chen et al., 2010). Electrostatic potential on the protein surface was calculated by APBS (v. 1.4) (Baker et al., 2001), and molecular graphics were created by PyMOL (v. 1.5) (DeLano, 2002).

Chemical Shift Perturbation Experiments

Chemical shift perturbation experiments were performed using a 0.1 mM ^{15}N-labeled SPOC domain in the NMR sample buffer described above. Unlabeled SMRT peptide (24-residue w/wo phosphorylations and 5- and 8-residue

with phosphoryaltions) were added stepwise up to an unlabeled-to-labeled sample ratio of two equivalents. The ^{15}N, HN chemical shift changes in the SPOC domain were monitored in ^{1}H-^{15}N HSQC spectra. δ_{ave} was calculated as $\{[\delta_{1H}{}^2 + 0.14(\delta_{15N})^2]\}^{1/2}$, where δ_{1H} and δ_{15N} represent the difference in ppm between the free and complex forms (Williamson, 2013).

In Vitro Binding Assay

Equilibrium surface plasmon resonance (SPR) measurements were carried out using ProteOn XPR36 (BioRad). Biotinylated 24-residue human SMRT polypeptides (aa 2502–2525) of various phosphorylation patterns were purchased from TORAY Research Center. Peptides were coupled via the N-terminal biotin moiety to a ProteOn NLC sensor chip (BioRad). Purified proteins (300 nM–5 μM) were injected into both peptide-linked and nonlinked sensor chip channels for correction of background signals. All binding experiments were performed at 25°C with a flow rate of 10 ml/min in a buffer consisting of 10 mM HEPES (pH 7.4), 150 mM NaCl, 1 mM DTT, and 0.05% surfactant P20. Data were analyzed with ProteOn Manager Software. K_D values were obtained by taking an average of at least three independent measurements.

The affinity for the wild-type SPOC domain/p-SMRT-C8(YETL(pS)D(pS)E) interaction was also determined by isothermal titration calorimetry with a ITC-200 (GE Healthcare) at 20°C. Protein and p-SMRT-C8 were dialyzed extensively into HEPES buffer (pH 7.5), 1 mM DTT, and 0.1 mM EDTA. The protein (0.5–1.0 mM) was titrated into 0.05–0.1 mM SMRT peptide. Data were analyzed with Origin (v. 7.0) software. The affinity was estimated from the three independent experiments.

Repression Assay

MH100-tk-luc and pCMX-Gal4-DBD were a kind gift from Professor Evans R.M. (Salk Institute). The wild-type SPOC fragment was amplified by PCR and cloned into pCMX-Gal4-DBD. The Gal4DBD-SPOC fragment was then amplified from pCMX-Gal4-DBD-SPOC by PCR and cloned into the HA tag vector. Gal4DBD-SPOC mutant-HA expression vectors were created by inverted PCR and DpnI digestion of the template. MH100-tk-luc, pRL-CMV, and GAL4DBD-SPOC mutant expression vectors were transfected into CV-1 cells by Polyfect transfection reagent (QIAGEN) in accordance with the manufacturer's protocol. After 24 hr transfection, cells were lysed and firefly and Renilla luciferase activity were measured. Transfection efficiency was normalized by Renilla luciferase activity.

Immunofluorescence

The HA-tagged GAL4DBD-SPOC mutant expression vector was transfected into CV-1 cells (which were at approximately 60% confluency) using polyfect transfection reagent. After 24 hr, cells were fixed with 4% paraformaldehyde, permeabilized with 0.2% Triton X-100 in PBS, and immersed into 1% milk in PBS. After blocking, cells were incubated with mouse monoclonal anti-HA antibody (SIGMA) at room temperature (RT) for 1 hr, were washed with 0.1% Tween20 in PBS, and were incubated with Alexa 488-conjugated anti-mouse IgG (Invitrogen) at (RT) room temperature for 1 hr, followed by incubation with DAPI at RT for 5 min. Cells were finally analyzed by fluorescent microscopy (Leica).

Phosphorylation Assay

pFALG-SMRT-C was constructed by PCR using human SMRT (aa 2321–2525) from the cDNA mixture QUICK-Clone cDNAs (Clontech) and was cloned into pFLAG-CMV-2 (SIGMA). The S2522A mutation was introduced by inverted PCR into pFALG-SMRT-C and designated as pFALG-SMRT-C (S2552A). pFLAG-SMRT-C and pFLAG-SMRT-C (S2522A) were transfected into CV-1 cells using the Polyfect transfection reagent (QIAGEN). After 24 hr, cells were suspended in MEM-0.1% FCS, and the CK2 inhibitor tetrabromocinnamic acid (TBCA) (Calbiochem) in DMSO, was added (to a final concentration of 50 μM). After further incubation for 8 hr, the cells were finally harvested and lysed. Whole-cell lysates were analyzed by SDS-PAGE and immunoblotting using a mouse monoclonal antibody specific for the FLAG tag (Sigma) and HRP-anti-mouse Ig (DAKO). FLAG-SMRT-C was visualized by Clarity Western ECL Substrate (BioRad). To check the phosphorylation, treatment with phosphatase for the lysate by 5 U calf intestinal alkaline phosphatase (CIAP; Takara) for 15 min at 30°C was also performed.

ACCESSION NUMBERS

The RCSB PDB accession number for the atomic coordinates of the SPOC/p-SMRT-C8 complex in this paper is 2RT5.

SUPPLEMENTAL INFORMATION

Supplemental Information includes Supplemental Experimental Procedures and seven figures and can be found with this article online at http://dx.doi.org/10.1016/j.str.2013.10.007.

ACKNOWLEDGMENTS

We thank Professor R.M. Evans for the gift of MH100-tk-luc and pCMX-Gal4-DBD, Yoji Kondo for peptide synthesis, and Professor Peter Güntert for the use of CYANA (v. 3.0). We also thank Tsutomu Daito, Takeshi Kumagai, Dr. Masato Taoka, and Professor Toshiaki Isobe for their assistance with SPR measurements. This work was supported by a Grant-in-Aid for Young Scientists (21770120) from the Japan Society for the Promotion of Science and a Grant-in-Aid for Scientific Research on Innovative Areas, Structural Cell Biology, Transient Macromolecular Complex, and Protein Modifications in Pathogenic Dysregulation of Signaling from the MEXT (22121001, 22121002, 22121516, 24121722, and 25117723 to M.M.).

Received: April 30, 2013
Revised: September 6, 2013
Accepted: October 7, 2013
Published: November 21, 2013

REFERENCES

Archer, S.J., Ikura, M., Torchia, D.A., and Bax, A. (1991). An alternative 3D NMR technique for correlating backbone 15N with side-chain Hb resonances in larger proteins. J. Magn. Reson. *95*, 636–641.

Ariyoshi, M., and Schwabe, J.W. (2003). A conserved structural motif reveals the essential transcriptional repression function of Spen proteins and their role in developmental signaling. Genes Dev. *17*, 1909–1920.

Baker, N.A., Sept, D., Joseph, S., Holst, M.J., and McCammon, J.A. (2001). Electrostatics of nanosystems: application to microtubules and the ribosome. Proc. Natl. Acad. Sci. USA *98*, 10037–10041.

Brünger, A.T., Adams, P.D., Clore, G.M., DeLano, W.L., Gros, P., Grosse-Kunstleve, R.W., Jiang, J.S., Kuszewski, J., Nilges, M., Pannu, N.S., et al. (1998). Crystallography & NMR system: a new software suite for macromolecular structure determination. Acta Crystallogr. D Biol. Crystallogr. *54*, 905–921.

Cabrejos, M.E., Allende, C.C., and Maldonado, E. (2004). Effects of phosphorylation by protein kinase CK2 on the human basal components of the RNA polymerase II transcription machinery. J. Cell. Biochem. *93*, 2–10.

Chen, V.B., Arendall, W.B., 3rd, Headd, J.J., Keedy, D.A., Immormino, R.M., Kapral, G.J., Murray, L.W., Richardson, J.S., and Richardson, D.C. (2010). MolProbity: all-atom structure validation for macromolecular crystallography. Acta Crystallogr. D Biol. Crystallogr. *66*, 12–21.

Colley, S.M., and Leedman, P.J. (2011). Steroid receptor RNA activator - a nuclear receptor coregulator with multiple partners: insights and challenges. Biochimie *93*, 1966–1972.

Cooper, C., Vincett, D., Yan, Y., Hamedani, M.K., Myal, Y., and Leygue, E. (2011). Steroid receptor RNA activator bi-faceted genetic system: heads or tails? Biochimie *93*, 1973–1980.

Craft, J.W., Jr., and Legge, G.B. (2005). An AMBER/DYANA/MOLMOL phosphorylated amino acid library set and incorporation into NMR structure calculations. J. Biomol. NMR *33*, 15–24.

Darnell, J.E., Jr., Kerr, I.M., and Stark, G.R. (1994). Jak-STAT pathways and transcriptional activation in response to IFNs and other extracellular signaling proteins. Science *264*, 1415–1421.

DeLano, W.L. (2002). The PyMOL molecular graphics system. http://www.pymol.org/.

Duncan, J.S., Turowec, J.P., Vilk, G., Li, S.S., Gloor, G.B., and Litchfield, D.W. (2010). Regulation of cell proliferation and survival: convergence of protein kinases and caspases. Biochim. Biophys. Acta *1804*, 505–510.

Espinosa, L., Santos, S., Inglés-Esteve, J., Muñoz-Canoves, P., and Bigas, A. (2002). p65-NFkappaB synergizes with Notch to activate transcription by triggering cytoplasmic translocation of the nuclear receptor corepressor N-CoR. J. Cell Sci. *115*, 1295–1303.

Glover, J.N., Williams, R.S., and Lee, M.S. (2004). Interactions between BRCT repeats and phosphoproteins: tangled up in two. Trends Biochem. Sci. *29*, 579–585.

Grzesiek, S., Ikura, M., Clore, G.M., Gronenborn, A.M., and Bax, A. (1992). A 3D triple-resonance NMR technique for qualitative measurement of carbonyl-Hb J coplings in isotopically enriched protein. J. Magn. Reson. *96*, 215–221.

Hao, B., Oehlmann, S., Sowa, M.E., Harper, J.W., and Pavletich, N.P. (2007). Structure of a Fbw7-Skp1-cyclin E complex: multisite-phosphorylated substrate recognition by SCF ubiquitin ligases. Mol. Cell *26*, 131–143.

Herrmann, T., Güntert, P., and Wüthrich, K. (2002). Protein NMR structure determination with automated NOE assignment using the new software CANDID and the torsion angle dynamics algorithm DYANA. J. Mol. Biol. *319*, 209–227.

Homma, M.K., Li, D., Krebs, E.G., Yuasa, Y., and Homma, Y. (2002). Association and regulation of casein kinase 2 activity by adenomatous polyposis coli protein. Proc. Natl. Acad. Sci. USA *99*, 5959–5964.

Homma, M.K., Wada, I., Suzuki, T., Yamaki, J., Krebs, E.G., and Homma, Y. (2005). CK2 phosphorylation of eukaryotic translation initiation factor 5 potentiates cell cycle progression. Proc. Natl. Acad. Sci. USA *102*, 15688–15693.

Hong, S.H., and Privalsky, M.L. (2000). The SMRT corepressor is regulated by a MEK-1 kinase pathway: inhibition of corepressor function is associated with SMRT phosphorylation and nuclear export. Mol. Cell. Biol. *20*, 6612–6625.

Johnson, G.L., and Lapadat, R. (2002). Mitogen-activated protein kinase pathways mediated by ERK, JNK, and p38 protein kinases. Science *298*, 1911–1912.

Johnston, I.M., Allison, S.J., Morton, J.P., Schramm, L., Scott, P.H., and White, R.J. (2002). CK2 forms a stable complex with TFIIIB and activates RNA polymerase III transcription in human cells. Mol. Cell. Biol. *22*, 3757–3768.

Koradi, R., Billeter, M., and Wüthrich, K. (1996). MOLMOL: a program for display and analysis of macromolecular structures. J. Mol. Graph. *14*, 51–55, 29–32.

Kretzschmar, M., and Massagué, J. (1998). SMADs: mediators and regulators of TGF-beta signaling. Curr. Opin. Genet. Dev. *8*, 103–111.

Kubicek, K., Cerna, H., Holub, P., Pasulka, J., Hrossova, D., Loehr, F., Hofr, C., Vanacova, S., and Stefl, R. (2012). Serine phosphorylation and proline isomerization in RNAP II CTD control recruitment of Nrd1. Genes Dev. *26*, 1891–1896.

Lanz, R.B., Razani, B., Goldberg, A.D., and O'Malley, B.W. (2002). Distinct RNA motifs are important for coactivation of steroid hormone receptors by steroid receptor RNA activator (SRA). Proc. Natl. Acad. Sci. USA *99*, 16081–16086.

Laskowski, R.A., Rullmannn, J.A., MacArthur, M.W., Kaptein, R., and Thornton, J.M. (1996). AQUA and PROCHECK-NMR: programs for checking the quality of protein structures solved by NMR. J. Biomol. NMR *8*, 477–486.

Lin, C.Y., Navarro, S., Reddy, S., and Comai, L. (2006). CK2-mediated stimulation of Pol I transcription by stabilization of UBF-SL1 interaction. Nucleic Acids Res. *34*, 4752–4766.

Linge, J.P., Williams, M.A., Spronk, C.A., Bonvin, A.M., and Nilges, M. (2003). Refinement of protein structures in explicit solvent. Proteins *50*, 496–506.

Litchfield, D.W. (2003). Protein kinase CK2: structure, regulation and role in cellular decisions of life and death. Biochem. J. *369*, 1–15.

Meggio, F., and Pinna, L.A. (2003). One-thousand-and-one substrates of protein kinase CK2? FASEB J. *17*, 349–368.

Meinhart, A., and Cramer, P. (2004). Recognition of RNA polymerase II carboxy-terminal domain by 3′-RNA-processing factors. Nature *430*, 223–226.

Mikami, S., Kanaba, T., Ito, Y., and Mishima, M. (2013). NMR assignments of SPOC domain of the human transcriptional corepressor SHARP in complex with a C-terminal SMRT peptide. Biomol. NMR Assign. *7*, 267–270.

Milbradt, A.G., Kulkarni, M., Yi, T., Takeuchi, K., Sun, Z.Y., Luna, R.E., Selenko, P., Näär, A.M., and Wagner, G. (2011). Structure of the VP16 transactivator target in the mediator. Nat. Struct. Mol. Biol. *18*, 410–415.

Newberry, E.P., Latifi, T., and Towler, D.A. (1999). The RRM domain of MINT, a novel Msx2 binding protein, recognizes and regulates the rat osteocalcin promoter. Biochemistry *38*, 10678–10690.

Novikova, I.V., Hennelly, S.P., and Sanbonmatsu, K.Y. (2012). Structural architecture of the human long non-coding RNA, steroid receptor RNA activator. Nucleic Acids Res. *40*, 5034–5051.

Oberoi, J., Fairall, L., Watson, P.J., Yang, J.C., Czimmerer, Z., Kampmann, T., Goult, B.T., Greenwood, J.A., Gooch, J.T., Kallenberger, B.C., et al. (2011). Structural basis for the assembly of the SMRT/NCoR core transcriptional repression machinery. Nat. Struct. Mol. Biol. *18*, 177–184.

Olsen, J.V., Blagoev, B., Gnad, F., Macek, B., Kumar, C., Mortensen, P., and Mann, M. (2006). Global, in vivo, and site-specific phosphorylation dynamics in signaling networks. Cell *127*, 635–648.

Oswald, F., Kostezka, U., Astrahantseff, K., Bourteele, S., Dillinger, K., Zechner, U., Ludwig, L., Wilda, M., Hameister, H., Knöchel, W., et al. (2002). SHARP is a novel component of the Notch/RBP-Jkappa signalling pathway. EMBO J. *21*, 5417–5426.

Panova, T.B., Panov, K.I., Russell, J., and Zomerdijk, J.C. (2006). Casein kinase 2 associates with initiation-competent RNA polymerase I and has multiple roles in ribosomal DNA transcription. Mol. Cell. Biol. *26*, 5957–5968.

Pinna, L.A. (2002). Protein kinase CK2: a challenge to canons. J. Cell Sci. *115*, 3873–3878.

Sawatsubashi, S., Murata, T., Lim, J., Fujiki, R., Ito, S., Suzuki, E., Tanabe, M., Zhao, Y., Kimura, S., Fujiyama, S., et al. (2010). A histone chaperone, DEK, transcriptionally coactivates a nuclear receptor. Genes Dev. *24*, 159–170.

Shen, Y., Delaglio, F., Cornilescu, G., and Bax, A. (2009). TALOS+: a hybrid method for predicting protein backbone torsion angles from NMR chemical shifts. J. Biomol. NMR *44*, 213–223.

Shi, Y., Downes, M., Xie, W., Kao, H.Y., Ordentlich, P., Tsai, C.C., Hon, M., and Evans, R.M. (2001). Sharp, an inducible cofactor that integrates nuclear receptor repression and activation. Genes Dev. *15*, 1140–1151.

Vojnic, E., Mourão, A., Seizl, M., Simon, B., Wenzeck, L., Larivière, L., Baumli, S., Baumgart, K., Meisterernst, M., Sattler, M., and Cramer, P. (2011). Structure and VP16 binding of the Mediator Med25 activator interaction domain. Nat. Struct. Mol. Biol. *18*, 404–409.

Watson, P.J., Fairall, L., and Schwabe, J.W. (2012a). Nuclear hormone receptor co-repressors: structure and function. Mol. Cell. Endocrinol. *348*, 440–449.

Watson, P.J., Fairall, L., Santos, G.M., and Schwabe, J.W. (2012b). Structure of HDAC3 bound to co-repressor and inositol tetraphosphate. Nature *481*, 335–340.

Williamson, M.P. (2013). Using chemical shift perturbation to characterise ligand binding. Prog. Nucl. Magn. Reson. Spectrosc. *73*, 1–16.

Yaffe, M.B., and Smerdon, S.J. (2001). PhosphoSerine/threonine binding domains: you can't pSERious? Structure *9*, R33–R38.

You, S.H., Lim, H.W., Sun, Z., Broache, M., Won, K.J., and Lazar, M.A. (2013). Nuclear receptor co-repressors are required for the histone-deacetylase activity of HDAC3 in vivo. Nat. Struct. Mol. Biol. *20*, 182–187.

Zhou, Y., Gross, W., Hong, S.H., and Privalsky, M.L. (2001). The SMRT corepressor is a target of phosphorylation by protein kinase CK2 (casein kinase II). Mol. Cell. Biochem. *220*, 1–13.

